

TerDiT: Ternary Diffusion Models with Transformers

Xudong Lu¹ Aojun Zhou¹ Ziyi Lin³ Qi Liu^{2,3} Yuhui Xu² Renrui Zhang^{1,3}
 Yafei Wen⁴ Shuai Ren⁴ Peng Gao³ Junchi Yan^{2,3} Hongsheng Li^{1*}
¹CUHK MMLab ²Shanghai Jiao Tong University
³Shanghai AI Laboratory ⁴vivo AI Lab
 {luxudong@link, hqli@ee}.cuhk.edu.hk



Figure 1: Sample images (256×256) generated by the ternary DiT model with 4.2B parameters. Comparison with full-precision diffusion transformer models (DiT-XL/2 with 675M parameters and Large-DiT-4.2B with 4.2B parameters) are shown in Fig. 4.

Abstract

Recent developments in large-scale pre-trained text-to-image diffusion models have significantly improved the generation of high-fidelity images, particularly with the emergence of diffusion models based on transformer architecture (DiTs). Among these diffusion models, diffusion transformers have demonstrated superior image generation capabilities, boosting lower FID scores and higher scalability. However, deploying large-scale DiT models can be expensive due to their extensive parameter numbers. Although existing research has explored efficient deployment techniques for diffusion models such as model quantization, there is still little work concerning DiT-based models. To tackle this research gap, in this paper, we propose **TerDiT**, a quantization-aware training (QAT) and efficient deployment scheme for ternary diffusion models with transformers. We focus on the ternarization of DiT networks and scale model sizes from 600M to 4.2B. Our work contributes to the exploration of efficient deployment strategies for large-scale DiT models, demonstrating the feasibility of training extremely low-bit diffusion transformer models from scratch while maintaining competitive image generation capacities compared to full-precision models. Code will be available at <https://github.com/Lucky-Lance/TerDiT>.

*Corresponding Author

1 Introduction

The advancements in large-scale pre-trained text-to-image diffusion models [1, 2, 3, 4, 5] have led to the successful generation of images characterized by both complexity and high fidelity to the input conditions. Notably, the emergence of diffusion models based on transformer architecture (DiTs) [6] represents a significant stride in this research domain. Compared with other diffusion models, diffusion transformers have demonstrated the capability to achieve lower FID scores with higher computation Gflops [6]. Recent research highlights the remarkable image generation capabilities of diffusion transformer architecture, as demonstrated in methods like Stable Diffusion 3 [7], and its impressive performance in video generation, showcased by work such as Sora².

Given the impressive performance of diffusion transformer models, researchers are now increasingly delving into understanding the scaling law of these vision models [8], which resembles large language models (LLMs). For instance, the Stable Diffusion 3 provides trained DiT models across a spectrum of parameter sizes, from 800 million to 8 billion. Additionally, there is speculation among researchers that Sora might boast around 3 billion parameters. Given the enormous parameter numbers, deploying these DiT models can often be costly, especially on certain end devices.

To deal with the deployment dilemma, there have already been some works on the efficient deployment of diffusion models recently [9, 10, 11, 12], most of which focus on model quantization. However, as far as we are concerned, there are still two main shortcomings in current research. Firstly, while much attention has been given to quantizing U-Net-based diffusion models, the exploration of quantization methods for transformer-based diffusion models remains quite limited. Secondly, most prevailing approaches in the current literature heavily rely on post-training quantization (PTQ) techniques for model quantization [9, 11, 13, 14, 15], which leads to unacceptable performance degradation, particularly with extremely low bit width (e.g., 2-bit and 1-bit). However, the extremely low-bit quantization of neural networks is important as it can significantly reduce the computation resources required for deployment [16], especially for models with huge parameter sizes. During our research, we find that there is still no work considering the extremely low-bit quantization of DiT models.

To tackle these shortcomings, we propose to leverage the quantization-aware training (QAT) technique for the extremely low-bit quantization of large-scale DiT models. Low-bit QAT methods for large-scale models have been discussed in the LLM domain. Recent works observe that training large language models with extremely low-bit parameters (e.g., binary and ternary) from scratch can also lead to competitive performance [17, 18] compared with their full-precision counterparts. This indicates that there still exists significant precision redundancy in large-scale models, and implies the feasibility of the QAT scheme for large-scale DiT models.

In this paper, we focus primarily on ternary weight networks [19] and provide **TerDiT**, the first quantization scheme for DiTs to our best knowledge. Our method achieves quantization-aware training (weight-only) and efficient deployment for ternary diffusion transformer models. Different from the naive quantization of linear layers in LLMs and CNNs [18, 19], we find that the direct weight ternarization of the adaLN module [20] in DiT blocks [6, 21] leads to large dimension-wise scale and shift values in the normalization layer compared with full-precision models (due to weight quantization, gradient approximation), which result in slower convergence speed and poor model performance. Consequently, we propose a variant of adaLN by applying an RMS Norm [22] after the ternary linear layers of the adaLN module to effectively mitigate this training issue.

With this modification, we scale the parameters of the ternary DiT model from 600M (size of DiT-XL/2 [6]) to 4.2B (size of Large-DiT-4.2B [23]), finding that models with a larger number of parameters can converge to better results. We further employ existing 2-bit CUDA kernels to deploy the trained ternary DiT models, resulting in over a **tenfold** reduction in the model checkpoint size and about **sixfold** reduction in the inference memory consumption, while achieving competitive generation quality. The contributions are summarized as follows:

1. Inspired by the quantization-aware training scheme for low-bit LLMs, we study the QAT methods for ternary DiT models and introduce DiT-specific improvements for better training, which have not been explored in DiT literature.

² <https://openai.com/index/sora>

2. We scale ternary DiT models from 600M to 4.2B parameters, and further deploy the trained ternary DiT on GPUs based on existing 2-bit CUDA kernels, enabling the inference of a 4.2B DiT model with less than 3GB GPU memory.
3. Competitive evaluation results compared with full-precision models on the ImageNet [24] benchmark (image generation) showcase the effectiveness of our proposed TerDiT scheme.

To our best knowledge, our study is the first attempt to explore the quantization of DiT models. We focus on quantization-aware training and efficient deployment for large ternary DiT models, offering valuable insights for future research on deploying DiT models with extremely low-bit precision.

2 Related Works

Diffusion Models. Diffusion models have gained significant attention in recent years due to their ability to generate high-quality images and their potential for various applications. The concept of diffusion models was first introduced by [25], proposing a generative model that learns to reverse a diffusion process. This work laid the foundation for subsequent research in the field. [1] further extended the idea by introducing denoising diffusion probabilistic models (DDPMs), which have become a popular choice for image generation tasks. DDPMs have been applied to a wide range of domains, including unconditional image generation [1], image inpainting [26], and image super-resolution [27]. Additionally, diffusion models have been used for text-to-image synthesis, as demonstrated by the DALL-E model [28] and the Imagen model [5]. These models showcase the ability of diffusion models to generate highly realistic and diverse images from textual descriptions. Furthermore, diffusion models have been extended to other modalities, such as audio synthesis [29] and video generation [30], demonstrating their versatility and potential for multimodal applications.

Quantization of Diffusion Models. The quantization of diffusion models has been studied in recent years to improve the efficiency of diffusion models. Post-training quantization (PTQ) methods, such as those presented in [9, 11, 13, 14, 15], offer advantages in terms of quantization time and data usage. However, these methods often result in suboptimal performance when applied to low-bit settings. To address this issue, [31] proposes combining quantization-aware low-rank adapters (QALoRA) with PTQ methods, leading to improved evaluation results. As an alternative to PTQ, quantization-aware training (QAT) methods have been introduced specifically for low-bit diffusion model quantization [12, 32, 33, 34]. Despite their effectiveness, these QAT methods are currently only limited to small-sized U-Net-based diffusion models, revealing a research gap in applying QAT to large-scale DiT models. Further exploration of QAT techniques for large DiT models with extremely low bit width could potentially unlock even greater efficiency gains and enable the effective deployment of diffusion models in resource-constrained environments.

Ternary Weight Networks. Ternary weight networks [19] have emerged as a memory-efficient and computation-efficient network structure, offering the potential for significant reductions in inference memory usage. When supported by specialized hardware, ternary weight networks can also deliver substantial computational acceleration. Among quantization methods, ternary weight networks have garnered notable attention, with two primary approaches being explored: weight-only quantization and weight-activation quantization. In weight-only quantization, as discussed in [35], solely the weights are quantized to ternary values. On the other hand, weight-activation quantization, as presented in [36, 37], involves quantizing both the weights and activations to ternary values. Recent research has demonstrated the applicability of ternary weight networks to the training of large language models [18], achieving results comparable to their full-precision counterparts. Building upon these advancements, our work introduces, for the first time, quantization-aware training and efficient deployment schemes specifically designed for ternary DiT models. By leveraging the benefits of ternary quantization in the context of DiT models, we aim to push the boundaries of efficiency and enable the deployment of powerful diffusion models in resource-constrained environments, opening up new possibilities for practical applications.

3 TerDiT

In this section, we introduce TerDiT, a framework designed to conduct weight-only quantization-aware training and efficient deployment of large-scale ternary DiT models. We first give a brief review of diffusion transformer (DiT) models in Sec. 3.1. Then building upon the previous open-sourced

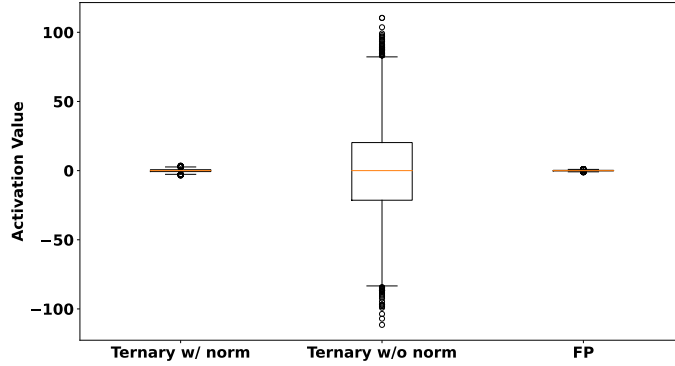


Figure 3: Activation value analysis. We compare activation values passing through a ternary weight linear layer with and without RMS Norm, using a full-precision linear layer as a reference. The ternary linear layer without RMS Norm results in extremely large activation values, introducing instability in neural network training. However, when the normalization layer is applied, the activation values are scaled to a reasonable range, similar to those observed in the full-precision layer.

each element by the average absolute value of all the elements in the matrix. After normalization, each value in the weight matrix is rounded to the nearest integer and clamped into the set $\{-1, 0, +1\}$.

Referring to current popular quantization methods for LLMs [41, 42], we also multiply a learnable scaling parameter α to each ternary linear matrix after quantization, leading to the final value set as $\{-\alpha, 0, +\alpha\}$. The quantization function is formulated as:

$$\widetilde{W} = \alpha \cdot \text{RoundClip}\left(\frac{W}{\gamma + \epsilon}, -1, 1\right), \quad (2)$$

where ϵ is set to a small value (e.g., 10^{-6}) to avoid division by 0, and

$$\text{RoundClip}(x, a, b) = \text{Clamp}(\text{round}(x), a, b) \text{ and } \gamma = \frac{1}{mn} \sum_{ij} |W_{ij}|. \quad (3)$$

TerDiT is a weight-only quantization scheme and we do not quantize the activations.

Quantization-aware Training Scheme. Based on the above-designed quantization function, we train a DiT model from scratch³ utilizing the straight-through estimator (STE) [43], allowing gradient propagation through the undifferentiable network components. We preserve the full-precision parameters of the network throughout the training process. For each training step, ternary weights are calculated from full-precision parameters by the ternary quantization function in the forward pass, and the gradients of ternary weights are directly applied to the full-precision parameters for parameter update in the backward pass.

However, we find the convergence speed is very slow. Even after many training iterations, the loss cannot be decreased to a reasonable range. We find that this issue may arise from the trait that ternary linear layers usually cause large activation values, and propose to tackle the problem with QAT-specific model structure improvement in the following subsection.

3.3 QAT-specific Model Structure Improvement

Activation Analysis for Ternary Linear Layer. In a ternary linear layer, all the parameters take one value from the set $\{-\alpha, 0, +\alpha\}$. The values passing through this layer would become large activation values, which might hamper the stable training of neural networks. We conduct a pilot study to qualitatively demonstrate the impact of ternary linear weights on activation values.

We randomly initialize a ternary linear layer with the input feature dimension set to 1024 and the output feature dimension to 9216 (corresponding to the linear layer of the adaLN module in Large-DiT). The weight parameters pass through the quantization function and receive a 512×1024 sized matrix input (filled with 1). The box plot of activation distribution is shown in the center part of Fig. 3. We also calculate the activation distribution after passing the matrix through a full-precision linear

³It is observed in [18] that for ternary LLMs, the conversion or post-training quantization from trained LLMs does not help. So we also train ternary DiT models from scratch.

layer generated with the same random seed, shown on the right part of Fig. 3. As can be seen, the ternary linear layer leads to very large activation values compared with full-precision linear layers.

The large-activation problem brought about by the ternary linear weights can be alleviated by applying a layer norm to the output of the ternary linear layer. We add an RMS Norm (similar to LLaMA) after the ternary linear layer and obtain the activation distribution (as shown in the left part of Fig. 3). In this case, the activation values are scaled to a reasonable range after passing the normalization layer and lead to more stable training behavior. The observation also aligns with [17], where a layer normalization function is applied before the activation quantization for each quantized linear layer.

RMS Normalized AdaLN Module. We analyze the DiT model for QAT-specific model structure improvement based on the above insights. In a standard ViT transformer block, the layer norm is applied for every self-attention layer and feedforward layer. This is also the case with the self-attention layers and feedforward layers in the DiT block, which can help to properly scale the range of activations. However, the DiT block differs from traditional transformer blocks due to the presence of the AdaLN module, as introduced in Sec. 3.1. Notably, there is no layer normalization applied to this module. In the context of full-precision training, the absence of layer normalization does not have a significant impact. However, for ternary DiT networks, its absence can result in large dimension-wise scale and shift values in the adaLN (normalization) module, posing bad influences on model training. To mitigate this issue, we introduce an RMS Norm after the MLP layer of the adaLN module in each ternary DiT block:

$$\text{adaLN_norm}(c) = \text{RMS}(\text{MLP}(\text{SiLU}(c))), \quad (4)$$

and the final model structure of TerDiT is illustrated in Fig. 2 (A). This minor modification can result in faster convergence speed and lower training loss, leading to better quantitative and qualitative evaluation results. To better showcase the effect, the actual activation distribution with/without the RMS Norm after model training is analyzed in Sec. A.1.

3.4 Deployment Scheme

After training the DiT model, we find that there are currently no effective open-source deployment solutions for ternary networks. In this case, we deploy the trained networks with a 2-bit implementation. To be specific, we pack the ternary linear weights to int8 values (4 ternary numbers into one int8 number) with the `pack_2bit_u8()` function provided by [44]. During the inference process of the DiT model, we call the complementary `unpack_2bit_u8()` function on the fly to recover packed 2-bit numbers to floating-point values, then perform subsequent calculations. The addition of the unpacking operation will slow down the inference process, but we believe that with further research into model ternarization, more hardware support for inference speedup will become available.

4 Experiments

In this section, a set of experiments are carried out to evaluate our proposed TerDiT. We show our main evaluation results in Sec. 4.1, carry out deployment efficiency comparison in Sec. 4.2, and illustrate the effectiveness of the RMS Normalized adaLN module in Sec. 4.3. Our DiT implementation is based on the open-sourced code of Large-DiT-ImageNet⁴. We conduct experiments on ternary DiT models with 600M (size of DiT-XL/2) and 4.2B⁵ (size of Large-DiT-4.2B) parameters respectively.

4.1 Main Evaluation Results

We provide quantitative and qualitative evaluation results of TerDiT in this subsection. To the best of our knowledge, there is no published work done on the quantization of diffusion transformer models at this point, so we mainly focus on the comparison with representative full-precision diffusion models in this subsection.

Remark on TerDiT Baselines. There is still no work studying the quantization of DiT models to our best knowledge. Other than comparison with full-precision models in this subsection, we have also established some baselines for comparison in other subsections. For the QAT baseline, we directly

⁴<https://github.com/Alpha-VLLM/LLaMA2-Accessory/tree/main/Large-DiT-ImageNet>

⁵The provided 3B model in the Large-DiT-ImageNet repository actually has 4.2B parameters.

ImageNet 256×256 Benchmark						
Models	Images (M)	FID ↓	sFID ↓	Inception Score ↑	Precision ↑	Recall ↑
BigGAN-deep [49]	-	6.95	7.36	171.40	0.87	0.28
StyleGAN-XL [50]	-	2.30	4.02	265.12	0.78	0.53
ADM [48]	507	10.94	6.02	100.98	0.69	0.63
ADM-U [48]	507	7.49	5.13	127.49	0.72	0.63
LDM-8 [4]	307	15.51	-	79.03	0.65	0.63
LDM-4 [4]	213	10.56	-	103.49	0.71	0.62
DiT-XL/2 (675M) [6]	1792	9.62	6.85	121.50	0.67	0.67
TerDiT-4.2B	604	9.66	6.75	117.54	0.66	0.68
Classifier-free Guidance						
ADM-G [48]	507	4.59	5.25	186.70	0.82	0.52
ADM-G, ADM-U [48]	507	3.94	6.14	215.84	0.83	0.53
LDM-8-G [4]	307	7.76	-	209.52	0.84	0.35
LDM-4-G [4]	213	3.60	-	247.67	0.87	0.48
DiT-XL/2-G (675M) [6]	1792	2.27	4.60	278.24	0.83	0.57
Large-DiT-4.2B-G	435	2.10	4.52	304.36	0.82	0.60
TerDiT-600M-G	448	4.34	4.99	183.49	0.81	0.54
TerDiT-4.2B-G	604	2.42	4.62	263.91	0.82	0.59

Table 1: Comparison between TerDiT and a series of full-precision diffusion models on the ImageNet 256×256 label-conditional generation task. For generation with classifier-free guidance, we use $\text{cfg}=1.5$. As can be seen, TerDiT achieves comparable results with full-precision models.

	Checkpoint Size	Memory Usage	Inference Time	FID-50k
DiT-XL/2-G	2.6GB	3921MiB	15s	2.27
Large-DiT-4.2B-G	16GB	17771MiB	83s	2.10
TerDiT-600M-G	168MB	1461MiB	20s	4.34
TerDiT-4.2B-G	1.1GB	3011MiB	97s	2.42

Table 2: Deployment efficiency comparison with $\text{cfg}=1.5$. TerDiT achieves a significant reduction in model size and memory usage while maintaining competitive evaluation results. Although the inference time of TerDiT is slightly slower due to the unpack operations, the inference time is expected to be significantly reduced with hardware support specifically designed for ternary models.

train the ternary DiT model without RMS Norm in the adaLN module in Sec. 4.3. To compare with existing PTQ [45] methods, we perform 4-bit weight quantization for pre-trained models on the same set of parameters as TerDiT, and find they just fail to generate viewable images (detailed in Sec. A.2).

Experiment Setup. Following the evaluation setting of the original DiT paper [6], we train 600M and 4.2B ternary DiT models on the ImageNet dataset. Due to computation resource limitations, we train and evaluate the model under 256×256 resolution, but we think that the evaluation results are already quite representative. We compare TerDiT with a series of full-precision diffusion models, report FID [46], sFID [47], Inception Score, Precision, and Recall (50k generated images) following [48]. We also provide the total number of images (million) during the training stage as in [23] to offer further insights into the convergence speed of different generative models.

Training Details. We train the 600M TerDiT model on 8 A100-80G GPUs for 1750k steps with batchsize set to 256, and the 4.2B model on 16 A100-80G GPUs for 1180k steps with batchsize set to 512. We set the initial learning rate as $5e-4$ ⁶. After 1550k steps of training for the 600M model and 550k steps for the 4.2B model, we reduce the learning rate back to $1e-4$ for more fine-grained parameter updates (ablation study on this learning rate reduction is provided in Sec. A.3).

Quantitative Results Analysis. The evaluation results are listed in Tab. 1. TerDiT is a QAT scheme for DiT models, so among all the full-precision models, we pay special attention to DiT-XL/2 (675M) and Large-DiT-4.2B. Without classifier-free guidance, TerDiT-4.2B achieves very similar testing results with DiT-XL/2 (with a much fewer number of training images). With classifier-free guidance

⁶The default learning rate of DiT is $1e-4$. In our experiments, we increase the initial learning rate to $5e-4$ following the observation in [17] that a larger learning rate is needed for the faster convergence of low-bit QAT.

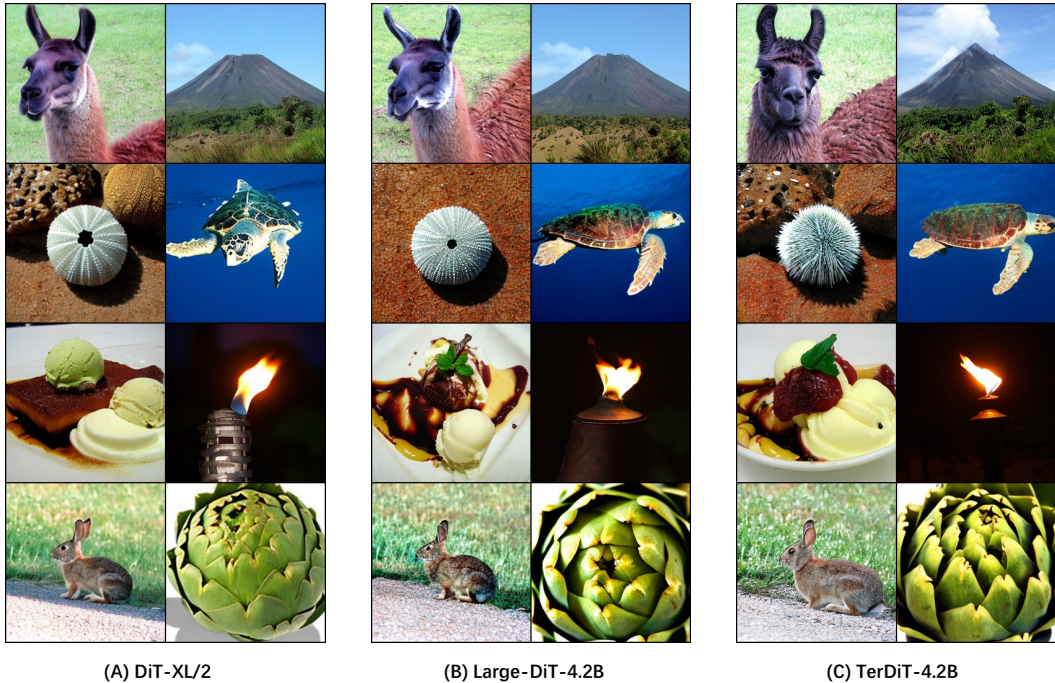


Figure 4: Qualitative results analysis. We compare images generated by DiT-XL/2 (A), Large-DiT-4.2B (B), and TerDiT-4.2B (C). We use class labels [355, 980, 328, 33, 928, 862, 330, 944] and $\text{cfg}=4$. TerDiT-4.2B can generate images of the same quality as the other two full-precision DiT models.

($\text{cfg}=1.5$), TerDiT-4.2B-G outperforms LDM-G while bringing a very slight performance degradation compared with two full-precision DiT-structured models. Besides, TerDiT-4.2B-G achieves better evaluation results than TerDiT-600M-G, implying that models with more parameters can incur smaller performance degradation after quantization.

Qualitative Results Analysis. To visually demonstrate the effectiveness of TerDiT, we also show some qualitative comparison results in Fig. 4, concerning TerDiT-4.2B, DiT-XL/2 and Large-DiT-4.2B. In terms of visual perception, there is no significant difference between the images generated by TerDiT and those generated by the full-precision models.

4.2 Deployment Efficiency Comparison

The improvement in deployment efficiency is the motivation of our proposed TerDiT scheme. In this subsection, we provide a comparison between TerDiT-600M/4.2B, DiT-XL/2, and Large-DiT-4.2B to discuss the actual deployment efficiency TerDiT can bring about. Tab. 2 shows the checkpoint sizes of the four DiT models. We also record the memory usage and inference time of the total diffusion sample loop ($\text{step}=250$) on a single A100-80G GPU.

From the table, we can see that TerDiT greatly reduces checkpoint size and memory usage. The checkpoint size and memory usage of the 4.2B ternary DiT model are significantly smaller than those of Large-DiT-4.2B, even smaller than DiT-XL/2. This brings significant advantages to deploying the model on end devices (e.g., mobile phones). We observe a slower inference speed due to the required unpack operations, but we believe that the computational advantage of ternary weight networks will be showcased through future hardware support.

4.3 Discussion on the RMS Normalized AdaLN Module

The main modification of TerDiT to the structure of the DiT model is the addition of an RMS Norm after the MLP in the adaLN module. In this part, we compare with the baseline ternary model to demonstrate the influence of RMS Norm on both the training process and the training outcomes.

Experiment Setup. We train ternary DiT models with 600M and 4.2B parameters on the ImageNet [24] dataset in 256×256 resolution. For each parameter size, we train two models, one with RMS Norm in the adaLN module and one without (our baseline). We record the loss curves during training and measure the FID-50k score ($\text{cfg}=1.5$) every 100k training steps.

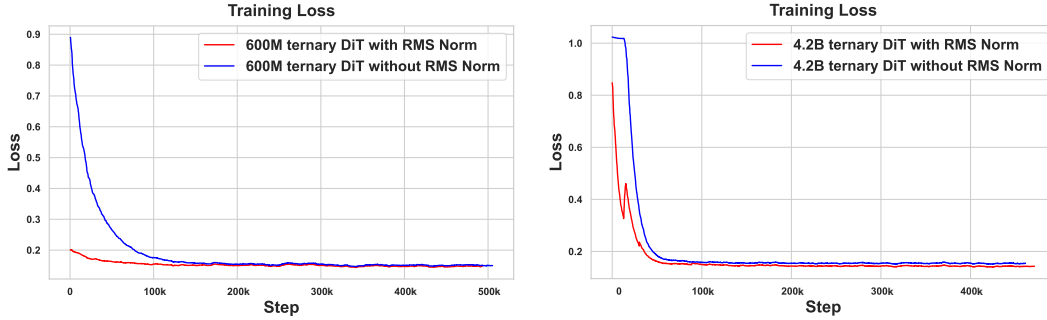


Figure 5: Training loss comparison of ternary DiT models with/without RMS Norm in the adaLN module. We show the loss curves training both 600M (left) and 4.2B (right) DiT models. Adding the RMS Norm will lead to faster convergence speed and lower training loss.

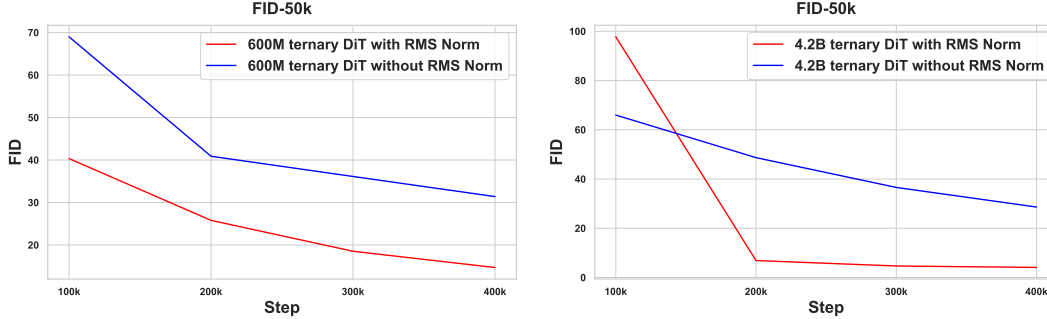


Figure 6: FID-50k score comparison on class-conditional ImageNet 256×256 generation task (cfg=1.5) with/without RMS Norm for both 600M and 4.2B ternary DiT models (100k steps to 400k steps). Training with RMS Norm will lead to lower FID scores.

Training Details. For a fair comparison, we train all the ternary DiT models on 8 A100-80G GPUs with batchsize set to 256. The learning rate is set to $5e-4$ throughout the training process.

Results Analysis. The training loss⁷ and evaluation scores are shown in Fig. 5 and Fig. 6 respectively. As can be seen, training with the RMS Normalized adaLN module will lead to faster convergence speed and lower FID scores. Another observation is that models with more parameters tend to achieve faster and better training compared to models with fewer parameters. This also to some extent reflects the scaling law of the ternary DiT model. Qualitative comparison results are shown in Sec. A.4.

5 Discussions and Future Works

In this paper, based on the successful low-bit training methods for large language models, we propose quantization-aware training (QAT) and efficient deployment methods for large-scale ternary DiT models. Competitive evaluation results on the ImageNet dataset (256×256) demonstrate the feasibility of training a large ternary DiT from scratch while achieving results comparable to those of full-precision models. To the best of our knowledge, this work is also the first study concerning the quantization of DiT models.

While we believe this work provides valuable insights into the low-bit quantization of DiT models, it still has some limitations. Firstly, training ternary DiT is less stable and more time-consuming than full-precision networks. In our paper, although we discuss how to make the training more stable by adding norms, it still remains more time-consuming than training full-precision networks (Large-DiT-4.2B), which will lead to an increase in carbon dioxide emissions during model training in a broader context. Secondly, limited by computational resource constraints, we do not conduct ImageNet 512×512 experiments, nor do we conduct experiments on the text-to-image generation task. However, we believe that the evaluation results on the ImageNet 256×256 benchmark are already quite representative. The remaining tasks will be reserved for our future work. We hope that our work can reduce the deployment requirements of image generation models, and can inspire the community to join us in the future, fostering a broader advancement of this field of study.

⁷The actual training process of diffusion models is not as ‘smooth’ as one might assume. To better illustrate the training dynamics, we employ exponential smoothing (with a smoothing factor of 0.995) during visualization.

References

- [1] Jonathan Ho, Ajay Jain, and Pieter Abbeel. Denoising diffusion probabilistic models. *Advances in Neural Information Processing Systems*, 33:6840–6851, 2020.
- [2] Jonathan Ho, Chitwan Saharia, William Chan, David J Fleet, Mohammad Norouzi, and Tim Salimans. Cascaded diffusion models for high fidelity image generation. *The Journal of Machine Learning Research*, 23(1):2249–2281, 2022.
- [3] Aditya Ramesh, Prafulla Dhariwal, Alex Nichol, Casey Chu, and Mark Chen. Hierarchical text-conditional image generation with clip latents, 2022. URL <https://arxiv.org/abs/2204.06125>, 7, 2022.
- [4] Robin Rombach, Andreas Blattmann, Dominik Lorenz, Patrick Esser, and Björn Ommer. High-resolution image synthesis with latent diffusion models. In *Proceedings of the IEEE/CVF conference on computer vision and pattern recognition*, pages 10684–10695, 2022.
- [5] Chitwan Saharia, William Chan, Saurabh Saxena, Lala Li, Jay Whang, Emily Denton, Seyed K Shayan Ghasemipour, Burcu Karagol Ayan, S Sara Mahdavi, Rapha Gontijo Lopes, et al. Photorealistic text-to-image diffusion models with deep language understanding. *arXiv preprint arXiv:2205.11487*, 2022.
- [6] William Peebles and Saining Xie. Scalable diffusion models with transformers. In *Proceedings of the IEEE/CVF International Conference on Computer Vision*, pages 4195–4205, 2023.
- [7] Patrick Esser, Sumith Kulal, Andreas Blattmann, Rahim Entezari, Jonas Müller, Harry Saini, Yam Levi, Dominik Lorenz, Axel Sauer, Frederic Boesel, et al. Scaling rectified flow transformers for high-resolution image synthesis. *arXiv preprint arXiv:2403.03206*, 2024.
- [8] Yixin Liu, Kai Zhang, Yuan Li, Zhiling Yan, Chujie Gao, Ruoxi Chen, Zhengqing Yuan, Yue Huang, Hanchi Sun, Jianfeng Gao, et al. Sora: A review on background, technology, limitations, and opportunities of large vision models. *arXiv preprint arXiv:2402.17177*, 2024.
- [9] Xiuyu Li, Yijiang Liu, Long Lian, Huanrui Yang, Zhen Dong, Daniel Kang, Shanghang Zhang, and Kurt Keutzer. Q-diffusion: Quantizing diffusion models. In *Proceedings of the IEEE/CVF International Conference on Computer Vision*, pages 17535–17545, 2023.
- [10] Yanyu Li, Huan Wang, Qing Jin, Ju Hu, Pavlo Chemerys, Yun Fu, Yanzhi Wang, Sergey Tulyakov, and Jian Ren. Snapfusion: Text-to-image diffusion model on mobile devices within two seconds. *Advances in Neural Information Processing Systems*, 36, 2024.
- [11] Yefei He, Luping Liu, Jing Liu, Weijia Wu, Hong Zhou, and Bohan Zhuang. Ptdq: Accurate post-training quantization for diffusion models. *Advances in Neural Information Processing Systems*, 36, 2024.
- [12] Haoxuan Wang, Yuzhang Shang, Zhihang Yuan, Junyi Wu, and Yan Yan. Quest: Low-bit diffusion model quantization via efficient selective finetuning. *arXiv preprint arXiv:2402.03666*, 2024.
- [13] Yuzhang Shang, Zhihang Yuan, Bin Xie, Bingzhe Wu, and Yan Yan. Post-training quantization on diffusion models. In *Proceedings of the IEEE/CVF Conference on Computer Vision and Pattern Recognition*, pages 1972–1981, 2023.
- [14] Yuewei Yang, Xiaoliang Dai, Jialiang Wang, Peizhao Zhang, and Hongbo Zhang. Efficient quantization strategies for latent diffusion models. *arXiv preprint arXiv:2312.05431*, 2023.
- [15] Changyuan Wang, Ziwei Wang, Xiuwei Xu, Yansong Tang, Jie Zhou, and Jiwen Lu. Towards accurate data-free quantization for diffusion models. *arXiv preprint arXiv:2305.18723*, 2(5), 2023.
- [16] Vivienne Sze, Yu-Hsin Chen, Tien-Ju Yang, and Joel S. Emer. Efficient processing of deep neural networks: A tutorial and survey. *Proceedings of the IEEE*, 105(12):2295–2329, 2017.
- [17] Hongyu Wang, Shuming Ma, Li Dong, Shaohan Huang, Huaijie Wang, Lingxiao Ma, Fan Yang, Ruiping Wang, Yi Wu, and Furu Wei. Bitnet: Scaling 1-bit transformers for large language models. *arXiv preprint arXiv:2310.11453*, 2023.
- [18] Shuming Ma, Hongyu Wang, Lingxiao Ma, Lei Wang, Wenhui Wang, Shaohan Huang, Li Dong, Ruiping Wang, Jilong Xue, and Furu Wei. The era of 1-bit llms: All large language models are in 1.58 bits. *arXiv preprint arXiv:2402.17764*, 2024.

- [19] Fengfu Li, Bin Liu, Xiaoxing Wang, Bo Zhang, and Junchi Yan. Ternary weight networks. *arXiv preprint arXiv:1605.04711*, 2016.
- [20] Ethan Perez, Florian Strub, Harm de Vries, Vincent Dumoulin, and Aaron C. Courville. Film: Visual reasoning with a general conditioning layer. In *AAAI Conference on Artificial Intelligence*, 2017.
- [21] Nanye Ma, Mark Goldstein, Michael S. Albergo, Nicholas M. Boffi, Eric Vanden-Eijnden, and Saining Xie. Sit: Exploring flow and diffusion-based generative models with scalable interpolant transformers, 2024.
- [22] Biao Zhang and Rico Sennrich. Root mean square layer normalization. In H. Wallach, H. Larochelle, A. Beygelzimer, F. d'Alché-Buc, E. Fox, and R. Garnett, editors, *Advances in Neural Information Processing Systems*, volume 32. Curran Associates, Inc., 2019.
- [23] Peng Gao, Le Zhuo, Ziyi Lin, Chris Liu, Junsong Chen, Ruoyi Du, Enze Xie, Xu Luo, Longtian Qiu, Yuhang Zhang, et al. Lumina-t2x: Transforming text into any modality, resolution, and duration via flow-based large diffusion transformers. *arXiv preprint arXiv:2405.05945*, 2024.
- [24] Jia Deng, Wei Dong, Richard Socher, Li-Jia Li, Kai Li, and Li Fei-Fei. Imagenet: A large-scale hierarchical image database. In *2009 IEEE conference on computer vision and pattern recognition*, pages 248–255. Ieee, 2009.
- [25] Jascha Sohl-Dickstein, Eric A Weiss, Niru Maheswaranathan, and Surya Ganguli. Deep unsupervised learning using nonequilibrium thermodynamics. *arXiv preprint arXiv:1503.03585*, 2015.
- [26] Yang Song, Jascha Sohl-Dickstein, Diederik P Kingma, Abhishek Kumar, Stefano Ermon, and Ben Poole. Score-based generative modeling through stochastic differential equations. *arXiv preprint arXiv:2011.13456*, 2020.
- [27] Chitwan Saharia, Jonathan Ho, William Chan, Tim Salimans, David J Fleet, and Mohammad Norouzi. Image super-resolution via iterative refinement. *arXiv preprint arXiv:2104.07636*, 2021.
- [28] Aditya Ramesh, Mikhail Pavlov, Gabriel Goh, Scott Gray, Chelsea Voss, Alec Radford, Mark Chen, and Ilya Sutskever. Zero-shot text-to-image generation. *arXiv preprint arXiv:2102.12092*, 2021.
- [29] Nanxin Chen, Yu Zhang, Heiga Zen, Ron J Weiss, Mohammad Norouzi, and William Chan. Wavegrad: Estimating gradients for waveform generation. *arXiv preprint arXiv:2009.00713*, 2020.
- [30] Jonathan Ho, Tim Salimans, Alexey Gritsenko, William Chan, Mohammad Norouzi, and David J Fleet. Video diffusion models. *arXiv preprint arXiv:2204.03458*, 2022.
- [31] Yefei He, Jing Liu, Weijia Wu, Hong Zhou, and Bohan Zhuang. Efficientdm: Efficient quantization-aware fine-tuning of low-bit diffusion models. *arXiv preprint arXiv:2310.03270*, 2023.
- [32] Xingyu Zheng, Haotong Qin, Xudong Ma, Mingyuan Zhang, Haojie Hao, Jiakai Wang, Zixiang Zhao, Jinyang Guo, and Xianglong Liu. Binarydm: Towards accurate binarization of diffusion model. *arXiv preprint arXiv:2404.05662*, 2024.
- [33] Yanjing Li, Sheng Xu, Xianbin Cao, Xiao Sun, and Baochang Zhang. Q-dm: An efficient low-bit quantized diffusion model. *Advances in Neural Information Processing Systems*, 36, 2024.
- [34] Hanwen Chang, Haihao Shen, Yiyang Cai, Xinyu Ye, Zhenzhong Xu, Wenhua Cheng, Kaokao Lv, Weiwei Zhang, Yintong Lu, and Heng Guo. Effective quantization for diffusion models on cpus. *arXiv preprint arXiv:2311.16133*, 2023.
- [35] Chenzhuo Zhu, Song Han, Huizi Mao, and William J Dally. Trained ternary quantization. *arXiv preprint arXiv:1612.01064*, 2016.
- [36] Hande Alemdar, Vincent Leroy, Adrien Prost-Boucle, and Frédéric Pétrot. Ternary neural networks for resource-efficient ai applications. In *2017 international joint conference on neural networks (IJCNN)*, pages 2547–2554. IEEE, 2017.
- [37] Peisong Wang, Qinghao Hu, Yifan Zhang, Chunjie Zhang, Yang Liu, and Jian Cheng. Two-step quantization for low-bit neural networks. In *Proceedings of the IEEE Conference on computer vision and pattern recognition*, pages 4376–4384, 2018.

- [38] Tero Karras, Samuli Laine, and Timo Aila. A style-based generator architecture for generative adversarial networks. In *Proceedings of the IEEE/CVF conference on computer vision and pattern recognition*, pages 4401–4410, 2019.
- [39] Hugo Touvron, Thibaut Lavril, Gautier Izacard, Xavier Martinet, Marie-Anne Lachaux, Timothée Lacroix, Baptiste Rozière, Naman Goyal, Eric Hambro, Faisal Azhar, et al. Llama: Open and efficient foundation language models. *arXiv preprint arXiv:2302.13971*, 2023.
- [40] Hugo Touvron, Louis Martin, Kevin Stone, Peter Albert, Amjad Almahairi, Yasmine Babaei, Nikolay Bashlykov, Soumya Batra, Prajjwal Bhargava, Shruti Bhosale, et al. Llama 2: Open foundation and fine-tuned chat models. *arXiv preprint arXiv:2307.09288*, 2023.
- [41] Elias Frantar, Saleh Ashkboos, Torsten Hoefler, and Dan Alistarh. Gptq: Accurate post-training quantization for generative pre-trained transformers. *arXiv preprint arXiv:2210.17323*, 2022.
- [42] Ji Lin, Jiaming Tang, Haotian Tang, Shang Yang, Xingyu Dang, and Song Han. Awq: Activation-aware weight quantization for llm compression and acceleration. *arXiv preprint arXiv:2306.00978*, 2023.
- [43] Yoshua Bengio, Nicholas Léonard, and Aaron Courville. Estimating or propagating gradients through stochastic neurons for conditional computation. *arXiv preprint arXiv:1308.3432*, 2013.
- [44] Hicham Badri and Appu Shaji. Half-quadratic quantization of large machine learning models, November 2023.
- [45] Guangxuan Xiao, Ji Lin, Mickael Seznec, Hao Wu, Julien Demouth, and Song Han. Smoothquant: Accurate and efficient post-training quantization for large language models. In *International Conference on Machine Learning*, pages 38087–38099. PMLR, 2023.
- [46] Martin Heusel, Hubert Ramsauer, Thomas Unterthiner, Bernhard Nessler, and Sepp Hochreiter. Gans trained by a two time-scale update rule converge to a local nash equilibrium. *Advances in neural information processing systems*, 30, 2017.
- [47] Tim Salimans, Ian Goodfellow, Wojciech Zaremba, Vicki Cheung, Alec Radford, and Xi Chen. Improved techniques for training gans. *Advances in neural information processing systems*, 29, 2016.
- [48] Prafulla Dhariwal and Alexander Nichol. Diffusion models beat gans on image synthesis. *Advances in neural information processing systems*, 34:8780–8794, 2021.
- [49] Andrew Brock, Jeff Donahue, and Karen Simonyan. Large scale gan training for high fidelity natural image synthesis. *arXiv preprint arXiv:1809.11096*, 2018.
- [50] Axel Sauer, Katja Schwarz, and Andreas Geiger. Stylegan-xl: Scaling stylegan to large diverse datasets. In *ACM SIGGRAPH 2022 conference proceedings*, pages 1–10, 2022.

A Appendix / supplemental material

A.1 Activation Distribution after Training

Here we conduct an analysis of the activation distribution during inference after model training, as a supplementary for the experiment and explanations in Sec. 3.3.

Following Sec. 4.3, we train the TerDiT-4.2B model with/without RMS Norm in the adaLN module for 50k steps. We then analyze the activation distribution of the ‘scale_mlp’ output in the adaLN module during inference, specifically at the first sampling step within the second ternary DiT block. For comparison, we also calculate the activation distribution of the original full-precision Large-DiT-4.2B model at the same layer. As shown in Fig. 7, training with RMS Norm can help limit the range of the activation values.

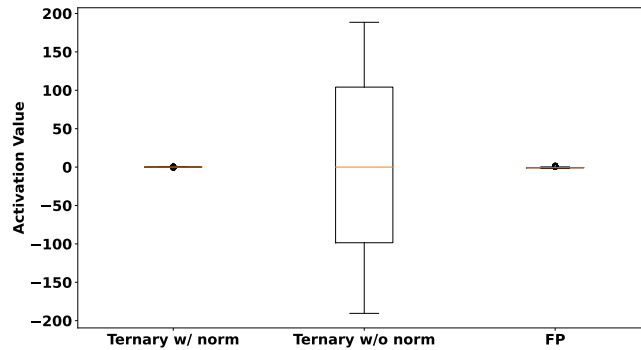


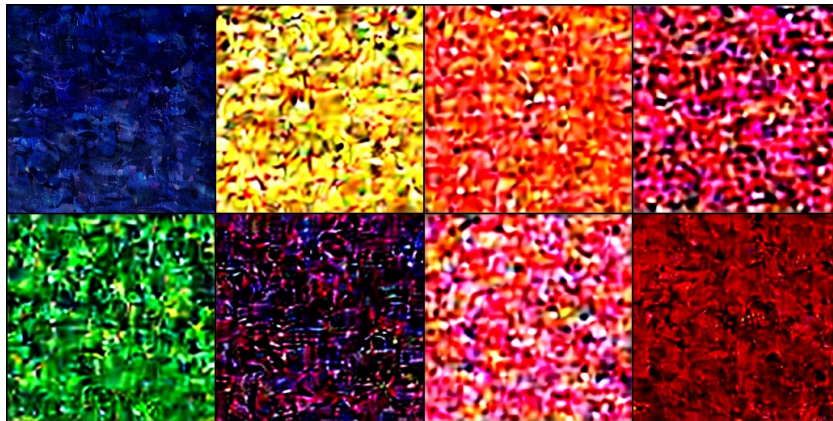
Figure 7: Activation value analysis. We train the TerDiT-4.2B model with/without RMS Norm in the adaLN module for 50k steps and show the activation distribution of the ‘scale_mlp’ output (one output of the adaLN module) in the second ternary DiT block during inference (at the first sampling step). The activation distribution of the original full-precision model is also provided.

A.2 Comparison with Existing PTQ Methods

For a simple comparison with PTQ methods, we adopt the fake quant function for model weight quantization⁸ provided in SmoothQuant [45] and set `n_bits=4`. We do not carry out activation quantization. Same as TerDiT, we quantize all the linear layer weights in self-attention, feedforward, and MLP of the original DiT blocks. We then sample images with the 4-bit quantized model. In this case, both original DiT-XL/2 and Large-DiT-4.2B fail to generate images. As shown in Fig. 8. However, TerDiT can generate high-quality images with ternary precision. This highlights the significance of QAT for extremely low-bit DiT quantization.



4-bit Large-DiT-4.2B



4-bit DiT-XL/2

Figure 8: DiT-XL/2 and Large-DiT-4.2B fail to generate images at 4-bit weight quantization.

⁸https://github.com/mit-han-lab/smoothquant/blob/main/smoothquant/fake_quant.py#L17

A.3 Effectiveness of Learning Rate Reduction

In Sec. 4.1, we adopt a learning rate reduction after training for certain steps for more fine-grained parameter updates. Here we provide an ablation study on this learning rate reduction.

We choose the TerDiT-600M model for convenience. Following the setting of Sec. 4.1, we train a TerDiT-600M model with RMS Normalized adaLN module and $5e-4$ learning rate for 1550k steps. We then continue training this model with $1e-4/5e-4$ for another 200k steps.

Quantitative Results. We evaluate FID, sFID, Inception Score, Precision, and Recall of these two models. As can be seen in Tab. 3, the reduction in learning rate will lead to better evaluation results.

ImageNet 256×256 Benchmark, Classifier-free Guidance						
Models	LR	FID ↓	sFID ↓	Inception Score ↑	Precision ↑	Recall ↑
TerDiT-600M-G (cfg=1.50)	$1e-4$	4.34	4.99	183.49	0.81	0.54
TerDiT-600M-G (cfg=1.50)	$5e-4$	6.38	5.00	147.79	0.76	0.54

Table 3: Effectiveness of learning rate reduction. Training with a reduced learning rate after 1550k steps for the TerDiT-600M model will lead to better evaluation results.

Qualitative Results. We also provide qualitative results comparison on TerDiT-600M with/without learning rate reduction in Fig. 9. For reference, the image generated by TerDiT-4.2B (fully trained) on the provided class label is shown in Fig. 10. The quality comparison highlights the importance of learning rate reduction in the later stages of training.



Figure 9: TerDiT-600M, class label [207, 360, 387, 974, 88, 979, 417, 279], cfg=4.



Figure 10: TerDiT-4.2B, class label [207, 360, 387, 974, 88, 979, 417, 279], cfg=4.

A.4 Qualitative Results Analysis for RMS Normalized AdaLN Module

In Sec. 4.3 we provide quantitative comparison results for models trained with/without RMS Norm in the adaLN module. Here we provide more qualitative results with models trained for 400k steps, together with the fully trained models.

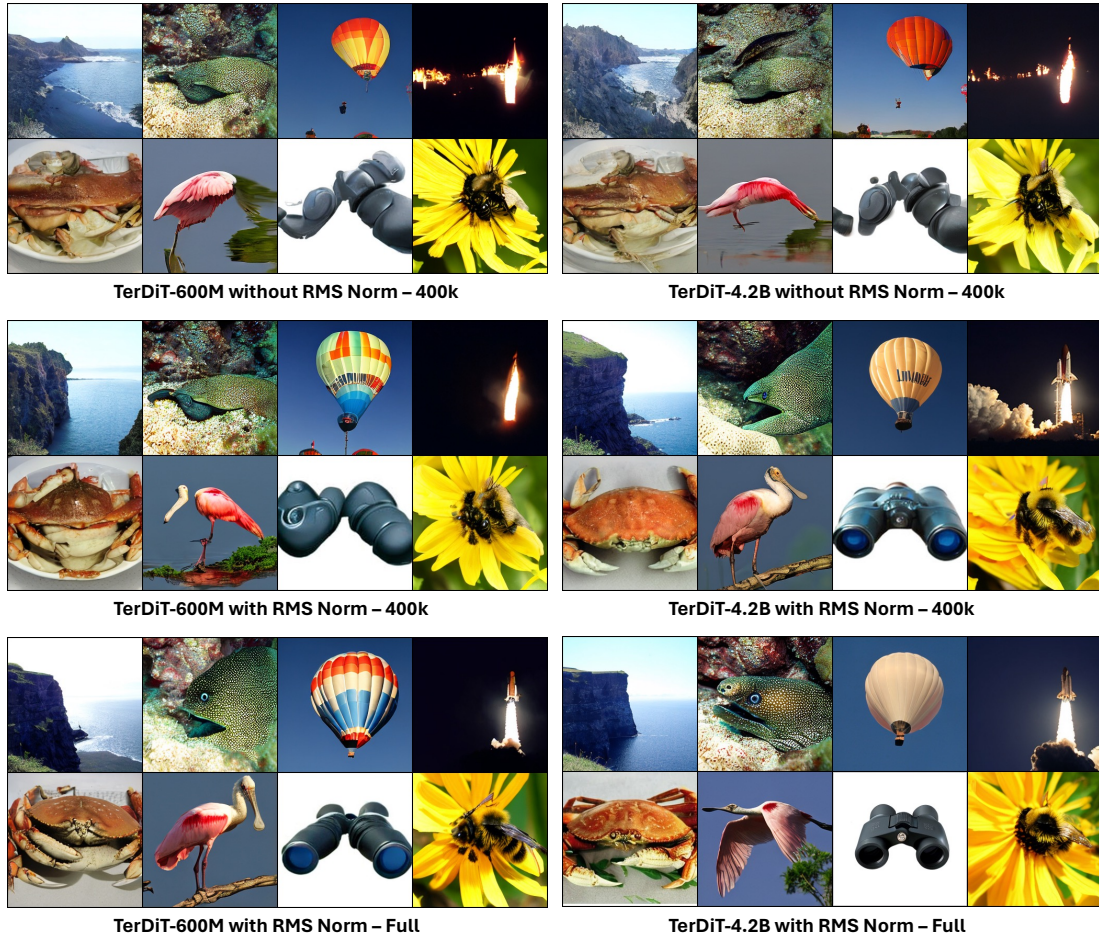


Figure 11: Qualitative results comparison for 600M and 4.2B ternary DiT models with/without RMS Norm in the adaLN module. We choose class labels [972, 390, 417, 812, 118, 129, 447, 309] with $\text{cfg}=4$. Training the 4.2B model with the RMS Normalized adaLN module will lead to better qualitative generation results.

We compare TerDiT-600M and TerDiT-4.2B models trained with/without RMS Norm in the adaLN module. We sample images from the models trained for 400k steps in Sec. 4.3 and also show the results of the fully trained models. The comparisons are demonstrated in Fig. 11.

We can come to two conclusions:

1. For both the 600M and 4.2B TerDiT model, training with the RMS Normalized adaLN module will lead to better qualitative results.
2. Models with more parameters show more learning ability and can achieve better training results compared to models with fewer parameters.

These observations are consistent with the quantitative results provided in Sec. 4.3.

A.5 More Qualitative Results



Figure 12: TerDiT-4.2B, class label [257, 300, 975, 973, 478, 388, 427, 809], cfg=4.



Figure 13: TerDiT-600M, class label [257, 300, 975, 973, 478, 388, 427, 809], cfg=4.